UMo/Al nuclear fuel plate behavior under thermal treatment (425-550°C)

H. Palancher[1,a)], A. Bonnin[1,2], C.V. Colin[3], V. Nassif[3], V. Honkimäki [2], R. Jungwirth[5], C. Ritter[4], G. Champion[1], Y. Calzavara[4].

[1] *CEA, DEN, DEC, Cadarache, F13108 Saint Paul lez Durance, France*

[2] *ESRF, BP 220, F38043 Grenoble Cedex, France*

[3] *Institut Néel, CNRS et Université Joseph Fourier, BP 166, 38042 Grenoble Cedex 9, France*

[4] *ILL, BP 156, 38042 Grenoble Cedex 9, France*

[5] *Forschungsneutronenquelle Heinz Maier-Leibnitz (FRM II), Technische Universität München, D-85747 Garching bei München, Germany*

[a)] Author to whom correspondence should be addressed. Electronic email: herve.palancher@cea.fr

Key words: neutron diffraction, synchrotron X-ray diffraction, in-situ, phase analysis, nuclear fuels

Abstract: Nuclear fuel plates based on a γU-Mo/Al mixture are proposed for research reactors. In this work their thermal behavior in the [425; 550°C] temperature range has been studied mainly by neutron and high energy X-ray diffraction. Even if complementary studies will be necessary, the kinetics of first the growth of the interaction layer between γU-Mo and Al and second of the γU-Mo destabilization have been accurately measured. This basic work should be helpful for defining manufacturing conditions for fuel plates with optimized composition.

1. INTRODUCTION

UMo/Al nuclear fuel plates proposed as a low enriched nuclear fuel for research reactors (such as neutron sources, material testing reactors) are manufactured by hot-rolling. Additional post-production thermal treatments (425-500°C) are currently envisaged for plates with optimized composition to improve their behavior under in-reactor irradiation (Yao *et al*., 2011; Keiser *et al*., 2011; Palancher, *et al*., 2012c). Duration for these annealings is limited by the growth of an UMo/Al interdiffusion layer (referred to as IL in the following). Indeed it may include crystallographic phases (i.e. $U_6Mo_4Al_{43}$ or UAl_4) with poor in-reactor performances (Gan *et al*., 2011).

Both composition and kinetics of growth for these ILs have been extensively studied on reference systems (UMo/Al diffusion couples) obtained at relative high temperatures (typically in the [550-600°C] range) (Mirandou *et al*., 2003; Palancher *et al*., 2007; Park *et al*., 2008; Perez, Keiser, Sohn, 2011). These works highlight the influence of the potential destabilization of the metastable γU-Mo phase in the analyzed sample. This phase may undergo a transformation towards either α-U and a γU-Mo phase enriched in Mo or α-U and U_2Mo (Massalski,1990).

The goal of the present work is to investigate both the IL characteristics (composition and growth kinetics) and γU-Mo phase stability at lower temperatures [425-550°C] on fuel plates themselves. In-situ neutron diffraction and ex-situ high energy X-ray diffraction (referred to as HE-XRD) measurements on annealed fuels have been used. Indeed this technique has been shown to be extremely powerful for characterizing these fuel plates and minor phases in the IL (Bonnin *et al*., 2011; Palancher, *et al*., 2012b; Palancher *et al*., 2012a; Jungwirth, *et al*., 2013). After having described the experimental procedure and the data analysis methodology, the obtained results are compared with those previously reported in the literature.

2. EXPERIMENTAL

A. Samples

In UMo/Al fuel plates the meat (containing the fissile part) is located inside both a frame and two sheets which act as a cladding.

https://doi.org/10.1017/S0885715613000894 Published online by Cambridge University Press

In the disperse case the meat is made of a dense mixture between Al (matrix) and γU-Mo powders. Mo is required for stabilization at room temperature of the high temperature cubic phase (γ) of metallic uranium. Indeed the U phases stable at lower temperatures i.e. α-U (from room temperature up to 667°C) and β-U (between 667 and 773°C) are orthorhombic and tetragonal respectively.

The samples analyzed in this work have been cut from the same UMo/Al full size plate manufactured by AREVA-CERCA (Romans, France). Note that the γU-Mo powder was produced by an atomisation process by the Korea Atomic Energy Research Institute (Daejon, South Korea) (Park *et al*., 2010). γU-Mo particles are therefore spherical and their diameter ranges between 20 and 120 μm. Their Mo content was 7 wt% (i.e. about 15 at%) and the uranium was depleted in ^{235}U (^{235}U<0.2wt%). Al alloys used in the meat and for the cladding were Al A5 and AG3NE respectively (Kapusta *et al*., 2003).

Post-manufacturing thermal treatment was performed at 425°C during two hours.
Fresh fuel plate was analyzed by HE-XRD and both optical and electron microscopy (Bonnin *et al*., 2011): the presence of impurity phases both in particles (UO_2, UC or UO) and in the matrix (UAl_4) has been reported.

Fuel plate pieces were mechanically polished either on one (for D1A neutron diffraction measurements) or two faces (for D1B experiments) to remove the Al cladding (cf. section 2.B). After having performed neutron diffraction experiments during thermal annealing, HE-XRD patterns on the annealed samples have been collected. Note that for the HE-XRD experiments, all samples were fully uncladded. In other words only the meat has been characterized.

B. Neutron diffraction experiments

Two kinds of neutron diffraction measurements are reported in this paper. Both of them have been performed at the Institut Laue Langevin (Grenoble, France).

https://doi.org/10.1017/S0885715613000894 Published online by Cambridge University Press

Firstly long duration isothermal studies were performed on the high flux two-axis D1B diffractometer. The wavelength was 2.52 Å, corresponding to the (002) Bragg reflection of a pyrolitic graphite monochromator. The harmonic at 1.26 Å could not be fully removed: the intensity of neutron beam with this wavelength is estimated to 0.3%. Diffraction data were collected using a curved position sensitive detector covering the [0.8; 128.8°] 2θ range i.e. [0.01; 0.35 $Å^{-1}$] sin θ/λ.

Samples were placed inside a vanadium can and in-situ measurements were performed under dynamic vacuum (10^{-4} mbar). Three temperatures (425, 450 and 475°C) have been studied during 52.7, 34.5, 13.8 hours respectively (cf. Figure I). Diffraction patterns were collected every 0.25 hour. Before and after the measurements in temperature, diffraction patterns were collected during 2 hours.

For each isothermal study, six pieces of fresh fully uncladded UMo/Al fuel plates (10×25×0.5 mm^3) have been loaded; this makes about 6 g of material (i.e. less than 5 g of U).

https://doi.org/10.1017/S0885715613000894 Published online by Cambridge University Press

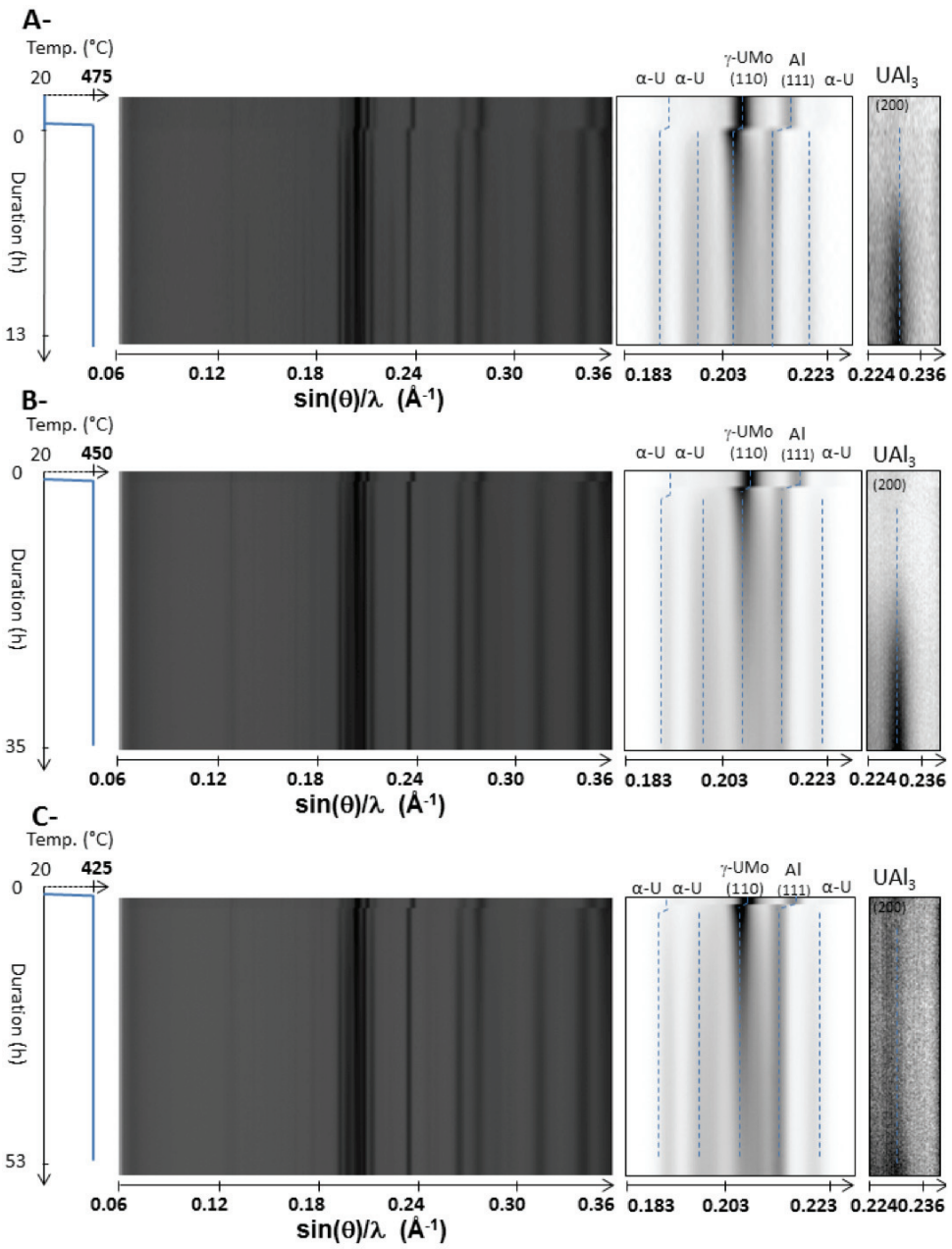

Figure I: In-situ neutron diffraction patterns (logarithmic scale) measured during isothermal annealing at 475°C (a-), 450°C (b-), 425°C (c-). On top of the full patterns, Two zooms highlight the evolution in the [0.183; 0.223] and [0.224; 0.236] sin θ/λ ranges enabling therefore the observation of γU-Mo destabilization and UAl_3 growth respectively. Fuel plate temperature is also indicated (left hand side).

Secondly experiments combining short duration thermal treatments and neutron diffraction measurements were performed on the high resolution two axis D1A diffractometer. Diffraction

https://doi.org/10.1017/S0885715613000894 Published online by Cambridge University Press

data were collected using a 1.90761 Å wavelength over a [20; 150°] 2θ i.e. [0.09; 0.51 $Å^{-1}$] sin θ/λ range. Fuel plates analyzed here were uncladded only on one side.

The experiment was performed in four steps using the same 3 g of material (i.e. 2.2 g of U): after having collected data at 20°C, temperature has been first increased up to 475°C and maintained to this value during 2 hours (first TT). Then heating was stopped and diffraction data were collected at 20°C. At a third step temperature has been set to 550°C during 4 hours (second TT). Finally samples were cooled down to 20°C and a last 4 hours neutron diffraction pattern has been collected.

In this paper, only the three patterns measured at 20°C before TT, after the first and the second TT will be considered. They are shown in Figure II.

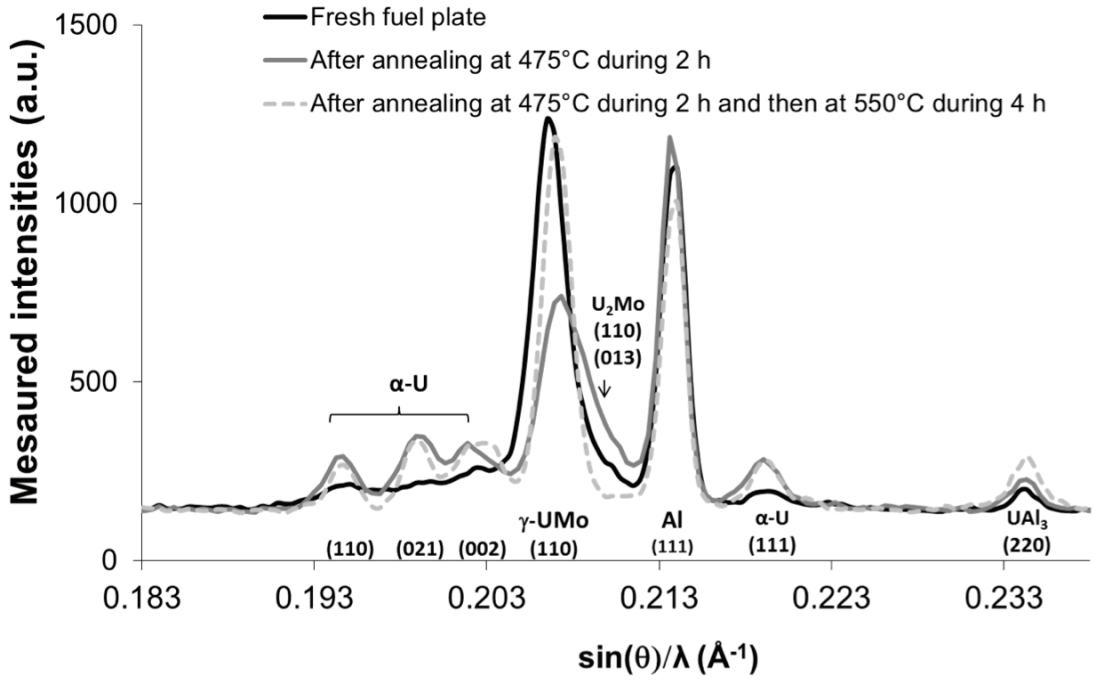

Figure II: Neutron diffraction patterns collected on the same samples (fuel plates) at 20°C before any annealing, after a 2h annealing at 475°C and after an additional annealing at 550°C during 4h.

C. High energy X-ray diffraction experiments

X-ray diffraction measurements at high energy (HE-XRD) have been carried out on the ID15B beamline at the ESRF (Grenoble, France). For these analyses, one piece of annealed fuel plate has been selected after each long duration isothermal treatment (at 425, 450 and 475°C) performed on D1B and after short duration thermal treatments on D1A (at 475°C during 2 hours

https://doi.org/10.1017/S0885715613000894 Published online by Cambridge University Press

and then at 550°C during 4 hours) (cf. section 2.B). Note that before HE-XRD analysis, samples taken from D1A experiment were mechanically polished to remove the remaining Al cladding (on one second side). This means that all HE-XRD experiments have been performed on meat samples.

A mapping has been performed at room temperature on each sample of interest with an X-ray beam size of 300×300 μm^2 at 87 keV. Each mapping gave about 140 2D diffraction patterns recorded each 40s, by a Pixium flat panel detector (by Thales). These patterns covering a [0.05; 11°] 2θ (i.e. [0.05; 0.62 $Å^{-1}$] sin θ/λ) range were then averaged and finally azimuthally integrated using the Fit2D software. As a conclusion the experimental procedure defined previously for fresh and thermally annealed fuel plates has been used (Bonnin *et al*., 2011).

3. DATA ANALYSIS

Diffraction patterns were analyzed using the Rietveld method and the FullProf software package. Pseudo-Voigt functions have been systematically chosen to simulate the Bragg line profile.

A. HE-XRD patterns

The analysis of HE-XRD patterns measured on γU-Mo/Al has been extensively described elsewhere (Bonnin *et al*., 2011; Palancher, *et al*., 2012b). The same eleven phases were used for these refinements: four for the U-Mo particle core (α-U, 2 γU-Mo phases, U_2Mo), two pollution phases (UO_2, UC or UO) around U-Mo particles, two for the matrix and impurity therein (Al, UAl_4) and three for the IL (UAl_3, UAl_2, $U_6Mo_4Al_{43}$).

The obtained crystallographic composition is given in Table I (the accuracy of this analysis is believed to be below 1 wt%) whereas α-U lattice constants are listed in Table II. The agreement between measured and calculated HE-XRD patterns can be seen in Figure III (agreement factors are given in Table III).

https://doi.org/10.1017/S0885715613000894 Published online by Cambridge University Press

Table I: Crystallographic composition of the four full size plates given by the Rietveld analysis of the HE-XRD and neutrons diffraction patterns measured on the same fuel plates at 20°C. Values are given in wt%. Moreover data related to the composition of the fuel plate annealed finally at 550°C during 4 hours are also mentioned for comparison.

		α-U	γU-Mo	UC	UO_2	U_2Mo	UAl_2	UAl_3	$U_6Mo_4Al_{43}$	Al	UAl_4
HE-XRD	fresh	23.1	61.7	0.6	0.3	4.1	---	---	---	10.5	0.1
	425	36.7	16.4	0.6	0.6	29.6	---	0.8	0	14.8	0.4
	450	38.7	14.4	0.7	0.4	24.9	0.2	9.9	1.95	8.1	1.4
	475	34.3	17.3	0.8	0.4	20.5	0.5	10.2	2.9	11.5	1.6
	550	24.5	43.1	0.3	0.3	---	1.2	14.6	4.7	10.9	--
Neutrons	fresh	17.5	56.3	--	0.2	11.6	---	---	---	14.5	---
	425	36.2	13.1	0	0.3	34.2	---	1.9	---	14.2	---
	450	33.5	14.2	0.2	0.2	32.0	---	10.3	---	9.7	---
	475	34.7	13.2	0.3	0.4	32.5	---	10.5	---	8.3	---

https://doi.org/10.1017/S0885715613000894 Published online by Cambridge University Press

Table II: Lattice constants for α'-U and α”-U measured at 20°C using HE-XRD.

	Thermal annealing conditions		α'-U lattice constants at 20°C (Å)			U crystallographic phase
	Temperature (°C)	Duration (h)	a	b	c	
γU-7Mo/Al	---	---	2.869	5.850	4.945	**α”**
	425	52.7	2.865	5.847	4.949	**α”**
	450	34.5	2.866	5.846	4.957	**α'**
	475	13.8	2.867	5.846	4.961	**α'**
	475 550	2 4	2.863	5.837	4.963	**α'**

Table III: Final agreement factors obtained for the refinement of HE-XRD and neutron diffraction patterns measured on annealed fuel plates.

	Thermal annealing conditions		Agreement factors (%)					
			HE-XRD			Neutron diffraction		
	Temperature (°C)	Duration (h)	R_p	R_{wp}	χ^2	R_p	R_{wp}	χ^2
γU-7Mo/Al	425	52.7	7.3	8.7	18.3	6.9	6.3	7.6
	450	34.5	6.11	7.3	14.4	7.7	8.6	8.0
	475	13.8	5.17	6.3	6.7	7.7	7.9	4.6

https://doi.org/10.1017/S0885715613000894 Published online by Cambridge University Press

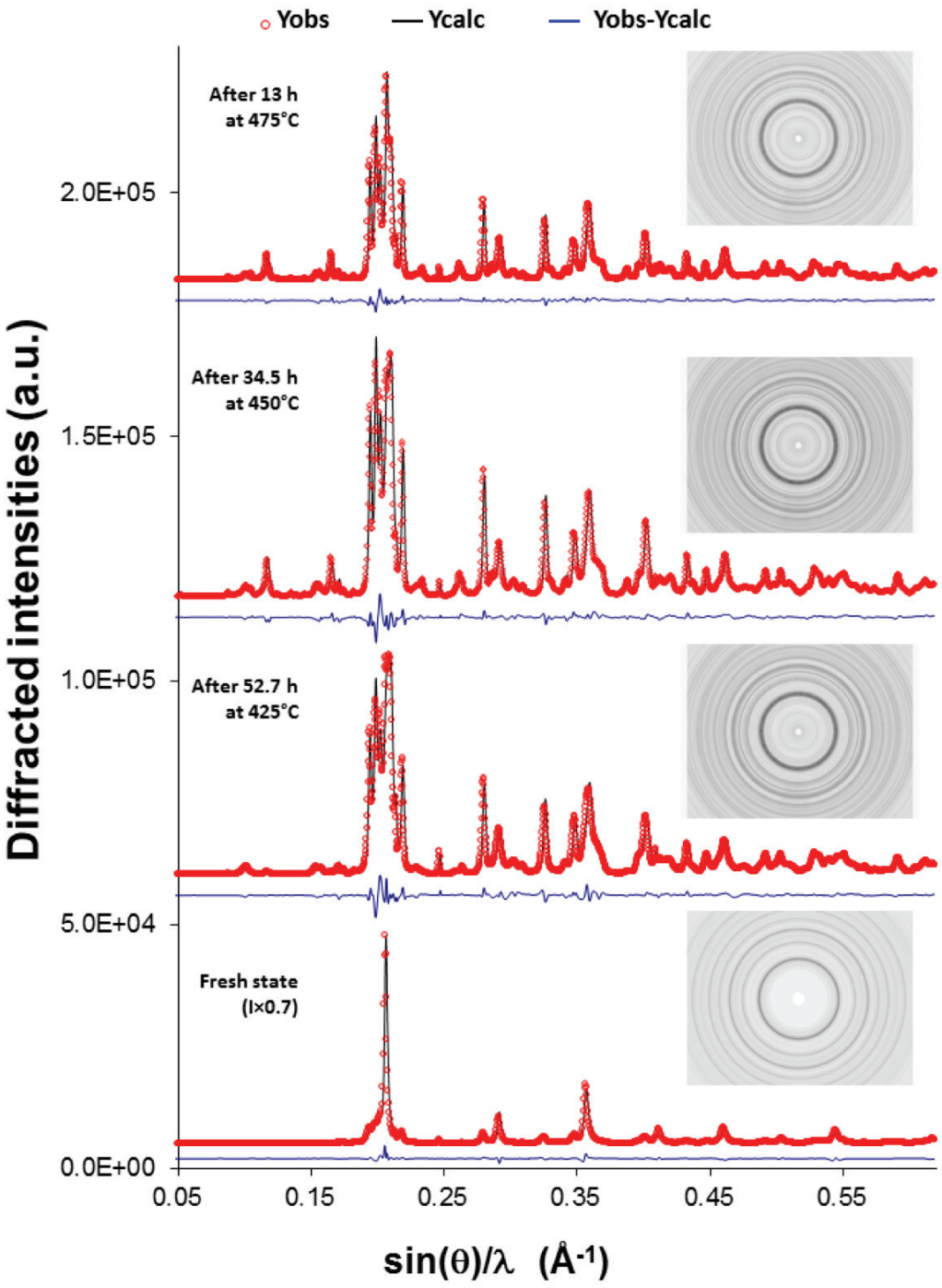

Figure III: Comparison between measured and calculated HE-XRD patterns before annealing and after three conditions of thermal treatments. Note that the Y-offset has been modified for patterns measured on annealed fuel plates and that intensities for the patterns measured on the fresh fuel plate (Bonnin *et al.*, 2011) has been multiplied by 0.7. The insets show the related 2D patterns. Measurements have been performed at 20°C.

https://doi.org/10.1017/S0885715613000894 Published online by Cambridge University Press

B. Neutron diffraction patterns

Whereas the three neutron diffraction patterns measured at room temperature on D1A have only been qualitatively interpreted (cf. Figure II), diffraction data collected on D1B during long isothermal treatments have been quantitatively analyzed.

In the Rietveld refinement of all patterns measured on D1B the same eight phases were used: four for the U-Mo particle core (α-U, two γU-Mo, U_2Mo), one for the matrix (Al), one for the IL (UAl_3) and two other pollution phases (UO_2, UC or UO). Indeed a lower signal to noise ratio (compared to HE-XRD) makes the identification of UAl_2, UAl_4 and $U_6Mo_4Al_{43}$ impossible. The analysis of neutron diffraction patterns was restricted to the [20; 150°] 2θ range.

Patterns measured at 20°C after the three thermal treatments (TT) have been first analyzed. The comparison between measured and calculated patterns for these three conditions is given in Figure IV. Final agreement factors for these refinements are listed in Table III. The analysis of the neutron diffraction patterns measured in-situ during TT is much more challenging. In addition to scale factors for the 8 phases, lattice constants for both α-U and the two U-Mo phases may also evolve during isothermal studies. As a consequence, these patterns have been automatically refined using a routine which enables a multi-step refinement (Palancher *et al*., 2011). At a first step, only scale factors of the eight phases were left free. Lattice constant were maintained fixed at the value refined on the pattern measured at the end of the TT. Obtained values for UAl_3, U_2Mo and Al are given in Table IV. Assuming a 23.5×10^{-6} K^{-1} thermal expansion factor for Al A5 alloy, Al lattice constants at 425, 450 and 475°C could be calculated. The comparison between measured and calculated Al lattice constants shows that lattice constants are given with accuracy better than 0.01 Å. At a second step, refined scale factor values have been fixed and only lattice constant for α-U and γU-Mo were optimized. At a last step, refinement of lattice constant was stopped and a new evaluation of scale factors for the eight phases has been performed.

https://doi.org/10.1017/S0885715613000894 Published online by Cambridge University Press

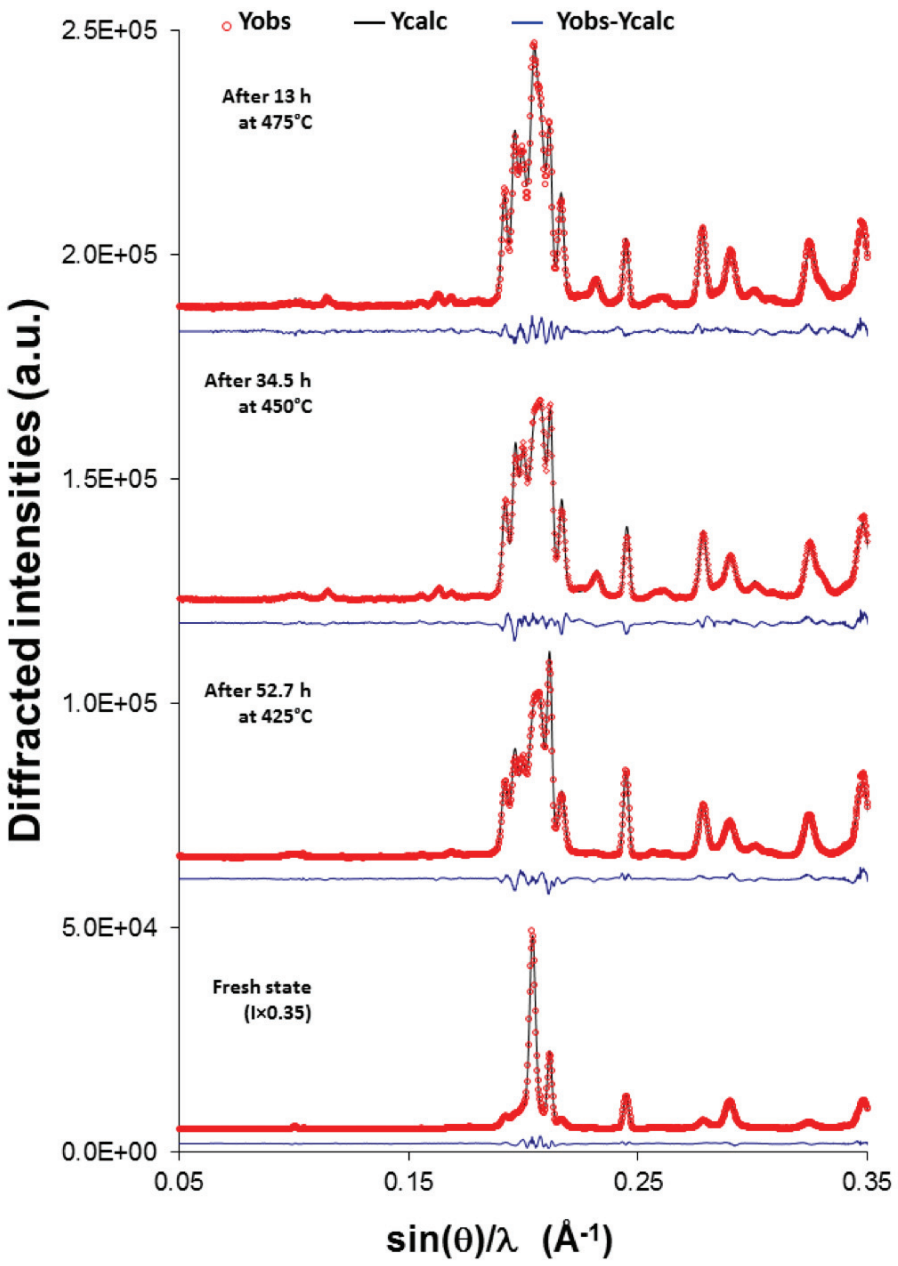

Figure IV: Comparison between measured and calculated neutron diffraction patterns before annealing and after three conditions of thermal treatments. Note that the Y-offset has been modified for patterns measured on annealed fuel plates and that intensities for the patterns measured on the fresh fuel plate have been multiplied by 0.35. Measurements have been performed at 20°C.

https://doi.org/10.1017/S0885715613000894 Published online by Cambridge University Press

Table IV: UAl_3, U_2Mo and Al lattice constant evolution with temperature

Temperature (°C)	Lattice constant (Å)				
	UAl_3	U_2Mo		Al	
		a	c	measurement	calculation
20	4.266	3.44	9.82	4.049	4.049
425				4.093	4.087
450				4.095	4.091
475	4.297	3.45	9.99	4.099	4.093

Comparing the high number of parameters to be refined to the number of measured Bragg lines (limited sin θ/λ range, high degree of overlap between Bragg lines), it becomes clear that all results of this analysis will not be robust. In particular, the evolution of γU-Mo and U_2Mo weight fractions appears to be strongly correlated and thus should not be quantitatively discussed. Regarding the cell parameter evolution, the three lattice constants for α-U are strongly correlated to the input model. As a consequence, the evolution of only three phases can be basically considered as robust i.e. UAl_3, α-U and Al.

4. RESULTS

Neutron diffraction and HE-XRD measurements can be directly compared since both of them lead to quantitative description of the crystallographic composition in γU-Mo/Al samples (Bonnin *et al.*, 2011). Furthermore in the experiments reported here, no sign of excessive fuel oxidation has been found (cf. Table I) thus confirming the relevance of the used experimental set-ups.

https://doi.org/10.1017/S0885715613000894 Published online by Cambridge University Press

A. Ex-situ high energy X-ray diffraction experiments

The efficiency of HE-XRD for characterizing both the IL crystallographic composition and the products of the γU-Mo destabilization must be again underlined.

As shown in Table I for the cases at 450 and 475°C, the IL consists of UAl_3, UAl_2 and $U_6Mo_4Al_{43}$, while UAl_4 is present initially as pollution inside the matrix (Bonnin *et al*., 2011). In contrast, at 425°C, only UAl_3 could be detected.

Concerning the behavior of the γU-Mo phase, it is shown here that it is transformed into a γU-Mo phase enriched in Mo (not discussed here), U_2Mo and a phase related to α-U. As demonstrated in Table II, this is α'-U at 550, 475 and 450°C whereas it is α”-U at 425°C (before and after annealing). Relationships between α-U lattice constants and crystallographic structure (and distortions) have been discussed in details previously (Tangri, Williams, 1961; Palancher, *et al.*, 2012b). Note that the presence of α”-U in the fresh fuel plate and in the plate annealed at 425°C during 52 hours, explains the higher values for agreement factors obtained at the end of the Rietveld refinements (cf. Table III). Indeed its crystal structure is not known with accuracy.

B. Neutron diffraction

In this section results obtained from D1B and D1A experiments are successively discussed.

Figure I shows the measured evolution of the (110) γU-Mo and (220) UAl_3 Bragg lines during the three TT performed on D1B. For these TT, the temperature increase induces a very fast decrease of the (110) γU-Mo Bragg line intensity when the increase of the UAl_3 (220) Bragg line is delayed. In other words the γU-Mo destabilization process occurs quicker than UMo/Al interaction, in the [425; 475°C] temperature range. Moreover the higher the annealing temperature, the quicker the growth of UAl_3. Figure V and Figure VI which show the UAl_3 and α-U weight fraction evolutions respectively obtained by Rietveld refinement, are in close

https://doi.org/10.1017/S0885715613000894 Published online by Cambridge University Press

agreement with this statement. Note that error bars in these figures which are given by the Rietveld refinement procedure, are probably underestimated.

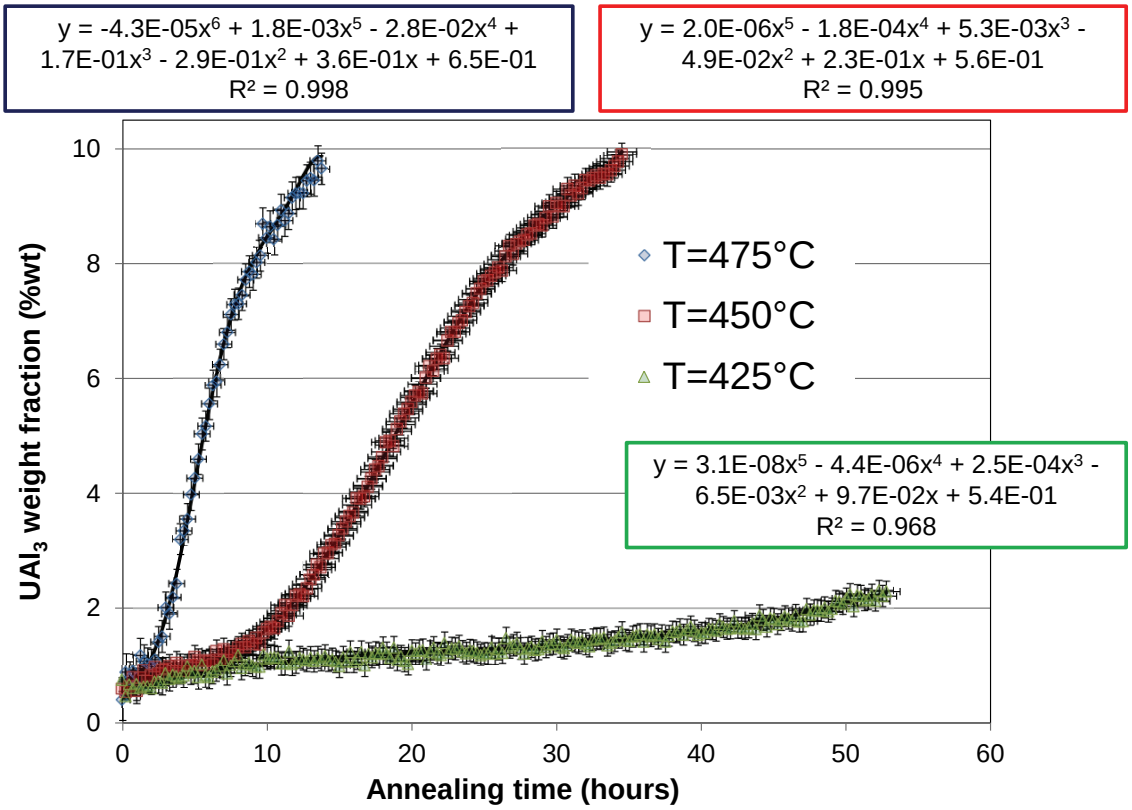

Figure V: UAl_3 growth kinetics as measured by in-situ neutron diffraction on γU-7Mo/Al samples as a function of annealing temperature (425, 450, 475°C)

https://doi.org/10.1017/S0885715613000894 Published online by Cambridge University Press

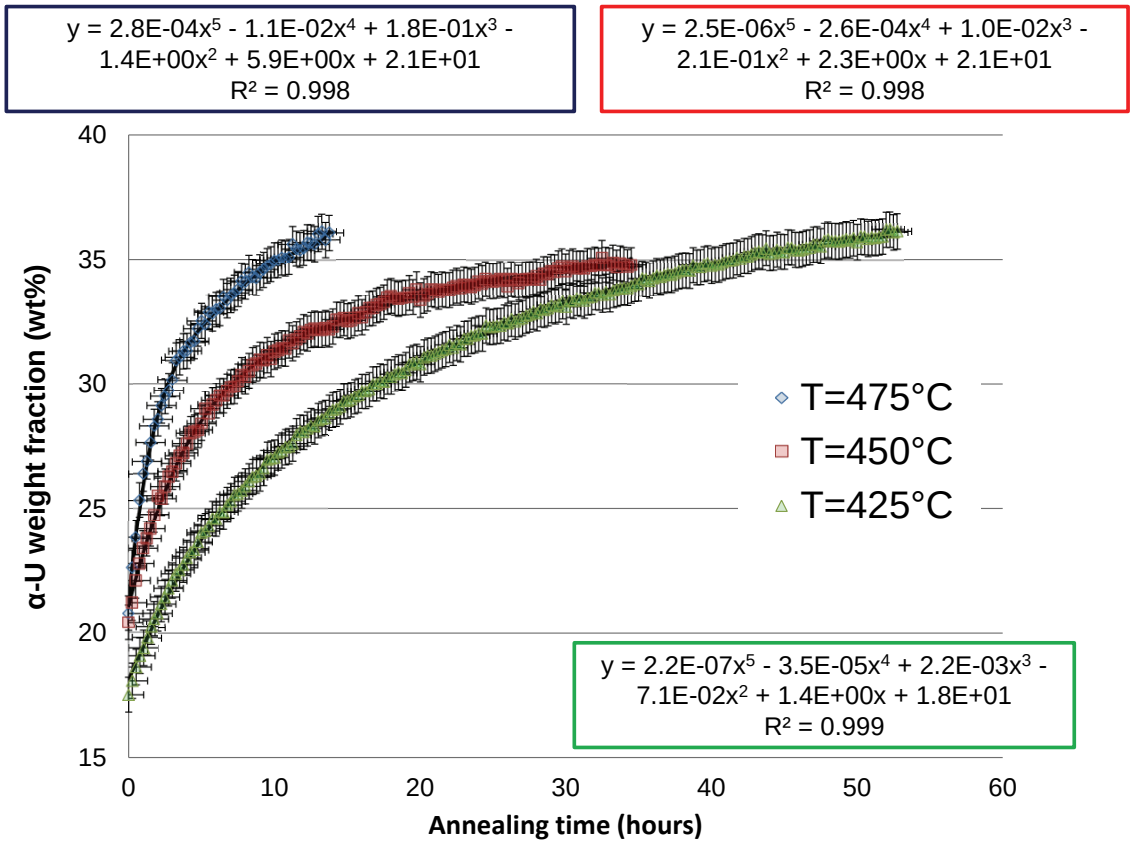

Figure VI: α'-U growth kinetics as measured by in-situ neutron diffraction on γU-7Mo/Al samples as a function of annealing temperature (425, 450, 475°C)

Comparing now neutron diffraction data collected on D1A and D1B on fresh samples, a good qualitative agreement can be observed except for Al Bragg line (cf. Figure II and Figure IV). Their intensity in D1A pattern is much larger; this was expected since the Al cladding has been removed on one side only for D1A whereas both sides have been uncladded for D1B measurements (cf. section 2.B).

The behavior after TT at 475°C during 2 hours performed on D1A is in excellent agreement with the one measured on D1B: transformation of the γU-Mo phase into U_2Mo and α'-U and beginning of the UMo/Al interaction. This can be seen by both a slight growth of the UAl_3 phase (see the increase of its (220) peak) and the strong decrease of the (110) γU-Mo intensity peak.

After the second annealing step (550°C during 4 hours) on D1A, an unexpected transformation of U_2Mo towards γU-Mo can be observed, α'-U weight fraction remaining almost constant. The absence of U_2Mo in this sample has also been confirmed by HE-XRD (cf. Table 1) (Bonnin *et*

https://doi.org/10.1017/S0885715613000894 Published online by Cambridge University Press

al., 2011). A re-stabilization of the γU-Mo phase has thus occurred. Note that its cell parameter is now different (3.417 Å) from the one measured on the fresh fuel plate (3.429 Å). This is associated to higher Mo content (Dwight, 1960; Park *et al*., 2010). Since γU-Mo Bragg lines are very sharp (cf. Figure II), it can be proposed that a recrystallization phenomenon has occurred at this temperature which is about one half of γU-Mo melting temperature. By recrystallization, Mo homogenization inside grains, annealing of defects due the manufacturing and even perhaps crystallite growth are meant. Moreover the UMo/Al interaction layer fraction has increased as demonstrated by the increase of the (220) UAl_3 Bragg line.

5. DISCUSSION

A. γU-Mo phase stability

At 425°C, the γU-Mo transformation has led to the growth of the U_2Mo and α"-U. This observation after more than 50 hours annealing is identical to the one made after 2 hours annealing.

At 450 and 475°C, the U_2Mo and α'-U phases are the products of the γU-Mo phase destabilization. The occurrence of such destabilization products (U_2Mo and α'-U) had also been characterized in fuel plates annealed at 475°C during 4 hours (Palancher, *et al.*, 2012b).
However it must be underlined that after a thermal annealing at 475°C during 2 hours, an additional thermal treatment at 550°C during 4 hours is efficient to fully convert the U_2Mo crystallographic phase into a γU-Mo phase. This can be described as a recrystallization mechanism.

Very recent analyses using transmission electron microscopy (TEM) performed on the UMo particles inside a UMo/AlSi fuel plate annealed at 425 or 475°C have demonstrated the presence of the β(UMo) phase (Yao *et al*., 2011). Here, no evidence for the presence of this high temperature phase has been found. It is likely that because of its very low weight fraction, this compound can only be detected using TEM.

B. IL characteristics

https://doi.org/10.1017/S0885715613000894 Published online by Cambridge University Press

1. Crystallographic composition

Table V recaps the IL crystallographic chemical composition and weight fraction inside the γU-Mo /Al meat as a function of annealing conditions. Two cases are presented there: results obtained on γU-7Mo/Al samples from this work and results obtained on γU-10Mo/Al by ex-situ neutron diffraction (Lee *et al.*, 2002). Considering the IL in γU-7Mo/Al samples, only results obtained with HE-XRD experiments are considered since they provide the highest accuracy. Indeed they evidence the presence of UAl_2 and $U_6Mo_4Al_{43}$ which do not appear on the neutron diffraction patterns (after isothermal treatment at 450°C and 475°C). The same results were obtained after the successive thermal treatments at 475 and 550°C (Bonnin *et al.*, 2011). This can be explained by the much lower signal to noise ratio in our neutron diffraction patterns (cf. section 3.B).

Table V: UMo/Al interaction layer (IL) weight fraction and crystallographic composition as a function of annealing conditions. For γU-7Mo/Al samples, only HE-XRD results are taken into account (cf. section 2.**A**).

	Thermal annealing conditions		IL weight fraction in the annealed U-Mo/Al sample (wt%)	IL crystallographic composition (wt%)		
	Temperature (°C)	Duration (h)		UAl_3	UAl_2	$U_6Mo_4Al_{43}$
γU-7Mo/Al	425	52.7	0.8	100	---	---
	450	34.5	12.1	82.2	1.6	16.2
	475	13.8	13.6	74.8	3.7	21.4
	475 550	2 4	>15	68.8	4.5	26.7
γU - 10Mo/Al (Lee *et al.*, 2002)	400	500	1.2	40	60	---
	400	1000	2.1	68.6	31.4	---
	500	100	5.2	60.6	39.4	---
	500	500	6.5	83.0	17.0	---

https://doi.org/10.1017/S0885715613000894 Published online by Cambridge University Press

It can be seen for γU-7Mo/Al samples that the IL weight fraction in the analyzed conditions is related first to temperature and second to the annealing duration: the largest IL fraction is obtained for the sample annealed at 475°C 2h and then 550°C 4h. Moreover the IL obtained in the [450; 550°C] temperature range has the same crystallographic composition: UAl_3 (69 to 82 wt%), UAl_2 (2 to 5 wt%) and $U_6Mo_4Al_{43}$ (16 to 27 wt%). After TT at 425°C, only UAl_3 has been found. However taking into account the very low weight fraction of this phase inside the analyzed sample (below 2 wt%) and the expected ratio between UAl_3 on the one hand and UAl_2 and $U_6Mo_4Al_{43}$ on the other hand, it cannot be excluded that UAl_2 and $U_6Mo_4Al_{43}$ are also present in the IL at this temperature. In other words, these phases would be present but in a too low amount to be seen in the HE-XRD pattern. This hypothesis should be validated by analyzing with HE-XRD a fuel plate containing a larger IL fraction after annealing at 425°C: duration ranging from 70 and up to 100 hours should be envisaged.
Based on these results, an IL composition averaged over annealing temperatures can be proposed (cf. Table V): 75 wt% UAl_3, 22 wt% $U_6Mo_4Al_{43}$ and 3 wt% UAl_2. It would be more difficult to discuss the influence of annealing temperature on this crystallographic chemical composition. However Table V suggests that by increasing annealing temperature the fraction of minor phases inside the IL (i.e. UAl_2 and $U_6Mo_4Al_{43}$) tends to increase (whereas the UAl_3 weight fraction decreases). This would have to be confirmed.

For γU-10Mo/Al samples, the IL obtained after annealing at 400°C during 1000 hours on the one hand and at 500°C during 100 and 500°C on the other hand (Lee *et al*., 2002) remains mainly made by UAl_3. Note that since the IL weight fraction is too limited (below 2wt%) in the sample annealed at 400°C during 500 hours, this sample has been disregarded. Only one minor phase (UAl_2) has however been found. It can be speculated that $U_6Mo_4Al_{43}$ has not been detected because of the lower signal-to-noise ratio in the measured neutron diffraction pattern.

Considering quantitatively the IL crystallographic composition obtained in γU-10Mo/Al samples, it appears that the UAl_2 fraction is higher significantly higher than obtained in this work for γU-7Mo/Al samples.

https://doi.org/10.1017/S0885715613000894 Published online by Cambridge University Press

To conclude, the crystallographic composition of the IL grown on γU-Mo/Al samples at temperatures in the [450-550°C] temperature range is made of the same phases: UAl_3, UAl_2, $U_6Mo_4Al_{43}$. With annealing temperature the ratios between each component evolve but UAl_3 remains the dominant crystallographic phase inside this IL.

2. Growth kinetics

UAl_3 growth kinetics at 425, 450 and 475°C have been first fitted using simple polynomial functions. These functions together with correlation factors are indicated in Figure V. It has been assumed that the initial offset of about 1 wt% in UAl_3 weight fraction has been created by the overlap between many UAl_3 peaks with other phases.

Considering that the crystallographic composition is constant with time and equals the values determined in section 5.B.1, the IL growth kinetics can be calculated: UAl_3 weight fractions have to be multiplied by a factor 1/0.75 to get the IL weight fraction. The obtained laws are reported in Table VI. Uncertainties associated with these IL fractions are estimated to 0.5 wt%. Therefore this work can be used to derive durations for which an IL has grown in γU-Mo /Al annealed fuel plates (i.e. durations for which the fitted IL weight fraction is larger than 0.5 wt%). These annealing durations are 2, 9 and 43 hours at 475°C, 450°C and 425°C respectively.

Table VI: UMo/Al interaction layer (IL) growth kinetics laws in γU-Mo7/Al nuclear fuel plates as a function of temperature.

Temperature (°C)	Coefficients for the IL polynomial growth law ($y= A\times t^6+ B\times t^5+ C\times t^4+ D\times t^3+ E\times t^2+F\times t+G$) in γU-Mo7/Al fuel plates (wt%)						
	A	B	C	D	E	F	G
425	-1.315 $\times10^{-10}$	2.534 $\times10^{-8}$	1.466 $\times10^{-6}$	4.175 $\times10^{-5}$	- 4.062 $\times10^{-4}$	2.155 $\times10^{-4}$	4.784 $\times10^{-2}$
450		2.266 $\times10^{-6}$	- 2.024 $\times10^{-4}$	5.658 $\times10^{-3}$	- 4.053 $\times10^{-2}$	8.221 $\times10^{-2}$	1.489 $\times10^{-1}$
475	-5.515 $\times10^{-5}$	2.299 $\times10^{-3}$	3.422 $\times10^{-2}$	2.015 $\times10^{-1}$	2.498 $\times10^{-1}$	1.807 $\times10^{-2}$	3.766 $\times10^{-1}$

https://doi.org/10.1017/S0885715613000894 Published online by Cambridge University Press

Finally by comparing for the three temperatures the IL growth kinetics (cf. Figure V) and an approximation of the γU-Mo destabilization kinetics (cf. Figure VI), one may conclude that both mechanisms are not correlated especially at 425°C. Much more work will be needed to compare these results with diffusivity values derived from SEM measurements on UMo/Al diffusion couples (Park *et al*., 2008). The main limitation of this work is related to the difficulty to accurately define annealing duration at which the IL starts to grow. To tackle this issue a complementary study should be undertaken combining *ex-situ* annealing experiments (for example 2, 8 and 24 hours at 475°C, 450°C and 425°C respectively) and characterizations with scanning electron microscopy (SEM) and HE-XRD. Indeed these techniques have a very low IL detection limit and therefore can be considered as probably more efficient than neutron diffraction for identifying the IL onset.

6. CONCLUSION

Studying real industrial materials using powder diffraction techniques is known to be very challenging: a dedicated methodology combining neutron diffraction and high energy X-ray diffraction had to be developed to characterize ex-situ and in-situ the thermal behavior of γU-Mo7/Al nuclear fuel plates.

Three main results have been obtained. Firstly the IL growth kinetics could be measured at three temperatures of industrial interest. Secondly, it has been shown that these kinetics are more influenced by temperature itself than by the γU-Mo7 particle destabilization level i.e. microstructure. Finally it has been shown that it is possible to at least partially restabilitize / homogenize γU-Mo7 particles inside a fuel plate: thermal annealing at 550°C (about one half of the γU-Mo7 melting temperature) has enabled the U_2Mo to γU-Mo transformation.

From a methodological point of view, in-situ neutron diffraction combined with HE-XRD has been shown to be very efficient for charactering the IL growth kinetics. This measurement could be even more fruitful if high $\sin(\theta)/\lambda$ neutron diffraction data could be collected. Indeed this would enable a more accurate study of destabilization kinetics for the γU-Mo7 phase. It should finally be mentioned that such a basic study would be best performed on pure γU-Mo7 samples (ingots, powder) rather than fuel plate (Champion *et al*., 2012). In fresh fuel plates γU-Mo

https://doi.org/10.1017/S0885715613000894 Published online by Cambridge University Press

particles already exhibit a significant level of destabilization: the very first stage of γU-Mo destabilization can therefore not be analyzed on these samples.

ACKNOWLEGMENT

C. TANGUY (CEA, DEC) is warmly thanked for her experimental and technical contribution to this work. The ESRF, CNRS and ILL are also acknowledged for providing beamtime.

Bonnin, A., Palancher, H., Honkimäki, V., Tucoulou, R., Calzavara, Y., Colin, C. V., Bérar, J-F., Boudet, N., Rouquette, H., Raynal, J., Valot, C. and Rodriguez-Carvajal, J. (**2011**). "UMo/Al nuclear fuel quantitative analysis via high energy X-ray diffraction," Z. Kristallogr. (Proceedings EPDIC 2010) **2011**, 29-34.

Champion, G., Belin, R., Palancher, H., Iltis, X., Rouquette, H., Pasturel, M., Demange, V., Castany, P., Dorcet, V. and Tougait, O. (**2012**). "Développement de méthodes de caractérisation sur poudres U(Mo), " Proceedings of the STP conference 2012, Toulouse (France)

Dwight, A. E. (**1960**). "The uranium -molybdenum equilibrium diagram below 900°C," J. Nucl. Mater. **2** 81-89.

Gan, J., Keiser Jr., D. D., Miller, B. D., Wachs, D. M., Allen, T. R., Kirk, M., Rest, J. (**2011**). "Microstructure of RERTR DU-alloys irradiated with krypton ions up to 100 dpa," J. Nucl. Mater. **411**, 174-180.

Jungwirth, R., Palancher, H., Bonnin, A., Bertrand-Drira, C., Borca, C., Honkimäki, V., Jarousse, C., Stepnik, B., Park, S.H., Iltis, X., Schmahl, W. and Petry, W. (**2013**) "Microstructure of as-fabricated UMo/Al(Si) plates prepared with ground and atomized powder," J. Nucl. Mater. **438**, 246–260.

Kapusta, B., Sainte-Catherine, C., Averty, X., Scibetta, M., Decroix, G. M., Rommens, M. (**2003**). Proceedings of the 9th IGORR conference, Sydney, Australia, March 24-28, 2003.

Keiser, D. D. Jr., Jue, J-F., Woolstenhulme, N. E. and Ewh, A. (**2011**). "Microstructural characterization of U–7Mo/Al–Si alloy matrix dispersion fuel plates fabricated at 500°C," J. Nucl. Mater. **419**, 226-234.

Lee J.-S., Lee C.-H., Kim K. H. and Em, V. (**2002**)**.** "Study of decomposition and reactions with aluminum matrix of dispersed atomized U-10 wt% Mo alloy," J. Nucl. Mater. **306**, 147-152.

Massalski, T. B. (**1990**). *Binary Alloy Phase Diagrams* (ASM International, Materials Park, OH), 2nd

Ed.

Mirandou, M. I., Balart, S. N., Ortiz, M., Granovsky, M. S. (**2003**). "Characterization of the reaction layer in U-7wt%Mo/Al diffusion couples," J. Nucl. Mater. **323**, 29-35.

Palancher, H., Martin, P., Nassif, V., Tucoulou, R., Proux, O., Hazemann, J-L., Tougait, O., Lahéra, E., Mazaudier, F., Valot, C. and Dubois, S. (**2007**). "Evidence for the presence of U-Mo-Al ternary compounds in the U-Mo/Al interaction layer grown by thermal annealing: A coupled micro X-ray diffraction and micro X-ray absorption spectroscopy study," J. Appl. Crystallogr. **40**, 1064-1075.

Palancher, H., Tucoulou, R., Bleuet, P., Bonnin, A., Welcomme, E. and Cloetens P. (**2011**). "Hard X-ray diffraction scanning tomography with sub-micrometre spatial resolution: application to an annealed γ-U0.85Mo0.15 particle," J. Appl. Crystallogr. **44**, 1111-1119.

Palancher, H., Bonnin, A., Honkimäki, V., Cloetens, P., Suhonnen, H., Zweifel, T., Tucoulou, R., Rack, A. and Voltolini, M. (**2012a**). "Coating thickness determination in highly absorbent core–shell systems," J. Appl. Crystallogr. **45**, 906-913.

Palancher, H., Bonnin, A., Honkimäki, V., Buslaps, T., Grasse, M., Stepnick, B., Zweifel, T. (**2012b**). "Quantitative crystallographic analysis of as-fabricated full size UMo/Al(Si) nuclear fuel plates," J. Alloys Compd. **527**, 53– 65.

Palancher, H., Iltis, X., Bonnin, A., Charollais, F., Lemoine, P., Van Den Berghe, S., Leenaers, A., Koonen, E., Stepnick, B., Jarousse, C., Calzavara, Y. and Guyon, H. (**2012c**). "LEONIDAS E-FUTURE-II: Characteristics of the fresh fuel plates," Proceedings of the 2012 RRFM Conference, Prague, Czech Republic, march 18-22, 2012, 709-718.

Park, J. M, Ryu, H. J., Oh, S. J., Lee, D. B., Kim C. K., Kim, Y. S., Hofman, G. L. (**2008**). "Effect of Si and Zr on the interdiffusion of U–Mo alloy and Al," J. Nucl. Mater. **374**, 422-430.

Park, J. M., Ryu, H. J., Kim, K. H., Lee, D. B, Lee, Y. S., Lee, J. S., Seong, B. S., Kim, C. K. and Cornen, M. (**2010**)." Neutron diffraction analyses of U–(6–10 wt.%)Mo alloy powders fabricated by centrifugal atomization," J. Nucl. Mater. **397**, 27–30.

Perez, E., Keiser, D. D., Jr. and Sohn, Y. H. (**2011**). "Phase Constituents and Microstructure of Interaction Layer Formed in U-Mo Alloys vs Al Diffusion Couples Annealed at 873 K (600 A degrees C)," Metall. Mater. Trans. A, **42**, 3071-3083.

Tangri, K., Williams, G. I. (**1961**). "Metastable phases in the uranium-molybdenum system and their origin," J. Nucl. Mater. **2**, 226-233.

Yao, B., Perez, E., Keiser, D. D. Jr., Jue, J.-F., Clark, C. R., Woolstenhulme, N., Sohn, Y. (**2011**). "Microstructure characterization of as-fabricated and 475 °C annealed U–7 wt.% Mo dispersion fuel in Al–Si alloy matrix," J. Alloys Compd. **509**, 9487– 9496.

https://doi.org/10.1017/S0885715613000894 Published online by Cambridge University Press